Available online at www.sciencedirect.com
SCIENCE DIRECT®
Catalysis Today 86 (2003) 191–209
CATALYSIS TODAY
www.elsevier.com/locate/cattod

Hydrodesulfurization over supported monometallic, bimetallic and promoted carbide and nitride catalysts

Brian Diaz, Stephanie J. Sawhill, Denise H. Bale, Rebekah Main, Diana C. Phillips, Scott Korlann, Randy Self, Mark E. Bussell*

Department of Chemistry, MS-9150, Western Washington University, 516 High Street, Bellingham, WA 98225-9150, USA

Received 11 March 2003; received in revised form 26 May 2003; accepted 26 May 2003

Abstract

The preparation of alumina-supported β-Mo_2C, MoC_{1-x} ($x \approx 0.5$), γ-Mo_2N, Co–Mo_2C, Ni_2Mo_3N, Co_3Mo_3N and Co_3Mo_3C catalysts is described and their hydrodesulfurization (HDS) catalytic properties are compared to conventional sulfide catalysts having similar metal loadings. Alumina-supported β-Mo_2C and γ-Mo_2N catalysts (Mo_2C/Al_2O_3 and Mo_2N/Al_2O_3, respectively) are significantly more active than sulfided MoO_3/Al_2O_3 catalysts, and X-ray diffraction, pulsed chemisorption and flow reactor studies of the Mo_2C/Al_2O_3 catalysts indicate that they exhibit strong resistance to deep sulfidation. A model is presented for the active surface of Mo_2C/Al_2O_3 and Mo_2N/Al_2O_3 catalysts in which a thin layer of sulfided Mo exposing a high density of sites forms at the surface of the alumina-supported β-Mo_2C and γ-Mo_2N particles under HDS conditions. Cobalt promoted catalysts, Co–Mo_2C/Al_2O_3, have been found to be substantially more active than conventional sulfided Co–MoO_3/Al_2O_3 catalysts, while requiring less Co to achieve optimal HDS activity than is observed for the sulfide catalysts. Alumina-supported bimetallic nitride and carbide catalysts (Ni_2Mo_3N/Al_2O_3, Co_3Mo_3N/Al_2O_3, Co_3Mo_3C/Al_2O_3), while significantly more active for thiophene HDS than unpromoted Mo nitride and carbide catalysts, are less active than conventional sulfided Ni–Mo and Co–Mo catalysts prepared from the same oxidic precursors.

Keywords: Carbides; Nitrides; Hydrodesulfurization; Thiophene

1. Introduction

Substantial improvements have been made in Mo sulfide-based hydrodesulfurization (HDS) catalysts since their inception into the industrial hydrotreating process nearly 60 years ago [1]. Over the last 30 years, nearly a 2-fold increase in HDS activity has been achieved [2]. Such improvements have allowed petroleum refineries to lower the sulfur content of transportation fuels in response to environmental regulations implemented in a number of countries. Given the likelihood of further reductions in the allowable sulfur content in fuels and the need to process lower quality petroleum feedstocks in future years, incremental improvements of Mo sulfide-based catalysts may not be sufficient to meet environmental standards.

To complement research efforts aimed at optimizing sulfide-based catalysts, many laboratories have adopted the approach of investigating how main group elements other than sulfur modify the catalytic properties of molybdenum. In this vein, molybdenum

* Corresponding author. Tel.: +1-360-650-3145; fax: +1-360-650-2826.
E-mail address: mark.bussell@wwu.edu (M.E. Bussell).

0920-5861/$ – see front matter © 2003 Elsevier B.V. All rights reserved.
doi:10.1016/S0920-5861(03)00411-5

carbide (β-Mo_2C) [3–9] and molybdenum nitride (γ-Mo_2N) [5,7,10–12] have attracted attention as potential catalysts for use in the HDS process. Interest in the catalytic properties of early transition metal carbides and nitrides for a variety of processes stems from the seminal research of Levy and Boudart [13], starting with a report that unsupported tungsten carbide (WC) catalyzed isomerization of neopentane. This isomerization reaction had been previously observed only for platinum and iridium catalysts [14]. Given that tungsten metal indiscriminately breaks the C–H and C–C bonds of hydrocarbon molecules adsorbed on its surface, the discovery that tungsten carbide is capable of the gentle chemistry required to catalyze hydrocarbon isomerization drew the strong notice of the catalysis community. The "platinum-like" catalytic behavior of tungsten carbide was rationalized as being the result of electron donation from carbon to tungsten upon alloying. By increasing the electron count of tungsten, its reactivity is moderated such that tungsten carbide exhibits catalytic properties similar to those of the group VIII elements located to its right in the periodic table [15,16]. The catalytic behavior of tungsten carbide and other transition metal carbides has been investigated for a number of other reactions and, in many cases, does in fact resemble that of group VIII metals [15,17]. High catalytic activities have also been measured for reactions catalyzed by metal nitrides; nitrogen has similar effects on the electronic properties of the associated metal as those of carbon in carbides [15,17]. For a more complete discussion of the chemistry of early transition metal carbides and nitrides as well as their catalytic properties for a range of applications, the reader is referred to excellent reviews published by others [17–19].

With respect to HDS catalysis, the "platinum-like" behavior of early transition metal carbides and nitrides attracted the interest of researchers because the sulfides of group VIII metals display HDS activities that are one to two orders of magnitude higher than those of the sulfides (Mo, W, Co, Ni) used in commercial HDS catalysts [20–22]. Indeed, a number of studies have shown alumina-supported molybdenum carbide (Mo_2C/Al_2O_3) [5–7] and molybdenum nitride (Mo_2N/Al_2O_3) [5,7,10–12] catalysts to be more active than conventional sulfided Mo/Al_2O_3 catalysts. In addition, the HDS properties of supported nitride catalysts containing Mo with either Co or Ni have been investigated and these catalysts have also been observed to have high HDS activities [23–25].

In this article, the HDS properties of supported carbides and nitrides are addressed, with particular focus on the synthesis, characterization and HDS evaluation studies carried out in our laboratory. Alumina-supported monometallic, bimetallic and promoted carbide and nitride catalysts are compared to conventional sulfide catalysts of similar metal composition, with the carbide and nitride catalysts generally exhibiting higher thiophene HDS activities. Based upon characterization studies, a model is presented to help understand the high HDS activities of the supported carbides and nitrides, but which does not invoke the "platinum-like" behavior that is often linked to the catalytic properties of early transition metal carbides and nitrides.

2. Experimental methods

2.1. Catalyst synthesis

2.1.1. MoO_3/Al_2O_3 and Mo_2C/Al_2O_3

Oxidic precursors (MoO_3/Al_2O_3) with theoretical loadings of 21 and 60 wt.% MoO_3 were synthesized according to previously published methods [5,7]. Finely ground gamma-alumina (γ-Al_2O_3, Engelhard Al-3945) was calcined at 773 K for 3 h in air, impregnated with aqueous solutions of ammonium heptamolybdate ($(NH_4)_6Mo_7O_{24}{\cdot}4H_2O$, Fisher, ACS grade), dried at 393 K, and then calcined at 773 K for 3 h in air.

Alumina-supported molybdenum carbide (Mo_2C/Al_2O_3) catalysts were prepared from oxidic precursors as described in detail elsewhere [5,7]. Approximately 1.5 g of the oxidic precursor was placed on a plug of quartz wool in a quartz U-tube. The oxidic precursor was degassed for 30 min at room temperature and then for 1 h at 673 K in 60 ml/min He (Airgas, 99.999% pure). The He was purified prior to use by passing it through 5 Å molecular sieve (Alltech) and O_2 (Oxyclear) purification traps. The temperature was ramped from 673 to 950 K at a rate of 30 K/h in a 30 ml/min flow of 20.0 mol% CH_4/H_2 mixture (Airgas, CH_4 99.8% pure, H_2 99 + % pure) and furnace-cooled to room temperature in the flowing CH_4/H_2 mixture. The CH_4/H_2 mixture was purified

in the same manner as was described for the He. Following temperature programmed reduction (TPR), the Mo_2C/Al_2O_3 catalysts were passivated in a 30 ml/min flow of a 1 mol% O_2/He mixture (Airgas, O_2 99% pure, He 99% pure) for 2 h at room temperature.

2.1.2. *Co–MoO_3/Al_2O_3 and Co–Mo_2C/Al_2O_3*

Promoted catalysts with theoretical Co/Mo molar ratios of 0.15, 0.31, 0.50, 0.75, and 1.0 were prepared by impregnation of MoO_3/Al_2O_3 (21 wt.% MoO_3) and 16 wt.% Mo_2C/Al_2O_3 catalysts with aqueous cobalt nitrate ($Co(NO_3)_2{\cdot}6H_2O$, Alpha Aesar, 99.5% pure). For X-ray diffraction (XRD) studies, a Co–Mo_2C/Al_2O_3 catalyst (Co/Mo = 0.28) was prepared by impregnation of a high loading MoO_3/Al_2O_3 (75 wt.% MoO_3) catalyst with $Co(NO_3)_2{\cdot}6H_2O$. The Co–MoO_3/Al_2O_3 and Co–Mo_2C/Al_2O_3 catalysts were transferred to a desiccator and dried under vacuum at room temperature. Following drying, the catalysts were passivated by back-filling the vacuum desiccator with 1 atm ($1\ \text{atm} = 1.013 \times 10^5$ Pa) of a 1 mol% O_2/He mixture for 2 h. The Co–Mo_2C/Al_2O_3 catalysts were not calcined following Co promotion to avoid oxidation of the supported β-Mo_2C particles. So that the catalyst preparation procedures were the same, the Co–MoO_3/Al_2O_3 catalysts also were not calcined following addition of the cobalt nitrate.

2.1.3. *Ni_2Mo_3N/Al_2O_3*

The synthesis of alumina-supported Ni_2Mo_3N has recently been described in detail elsewhere [26]. Alumina-supported oxidic precursors to Ni_2Mo_3N/Al_2O_3 catalysts with theoretical loadings of 10, 15, 20, 25, 30, and 50 wt.% Ni_2Mo_3N were prepared by impregnation of finely ground γ-Al_2O_3 with aqueous solutions of nickel nitrate ($Ni(NO_3)_2{\cdot}6H_2O$, Alfa Aesar, 99.9985% pure) and $(NH_4)_6Mo_7O_{24}{\cdot}4H_2O$, with drying at 393 K between impregnations, followed by calcination at 773 K for 2 h in air. The oxidic precursors (Ni/Mo = 0.67) were then nitrided according to the following procedure. Approximately 1.5 g of an oxidic precursor was degassed for 30 min at 295 K followed by 1 h at 393 K, both in 60 ml/min He (Airgas, 99.999% pure). The He was purified prior to use by passing it through 5 Å molecular sieve (Alltech) and O_2 (Oxyclear) purification traps. Following degassing, the sample was heated from 393 to 1173 K at a rate of 5 K/min in 30 ml/min ammonia (NH_3, Airgas, 99.99% pure) and the sample was then furnace-cooled to room temperature in the ammonia flow. The ammonia was purified in the same manner as was described above for the He. Following furnace cooling, the Ni_2Mo_3N/Al_2O_3 catalysts were passivated for 3 h in a 60 ml/min flow of 1 mol% O_2/He (Airgas) prior to air exposure.

2.1.4. *Co_3Mo_3N/Al_2O_3 and Co_3Mo_3C/Al_2O_3*

The synthesis of alumina-supported Co_3Mo_3N and Co_3Mo_3C catalysts has recently been described in detail elsewhere [26]. Alumina-supported oxidic precursors ($CoMoO_4/Al_2O_3$) to 20 wt.% Co_3Mo_3N/Al_2O_3 and Co_3Mo_3C/Al_2O_3 catalysts were prepared by impregnation of γ-Al_2O_3 with aqueous solutions of $Co(NO_3)_2{\cdot}6H_2O$ and $(NH_4)_6Mo_7O_{24}{\cdot}4H_2O$ followed by calcination in air. The alumina was calcined at 773 K for 3 h in air prior to impregnation. The impregnated samples were dried at 373 K and then calcined at 773 K for 3 h in air. Approximately 1.0 g of an oxidic precursor was degassed for 1 h at 295 K in 60 ml/min He and then heated from 295 to 1023 K at a rate of 2 K/min in 60 ml/min NH_3. The Co_3Mo_3N/Al_2O_3 catalyst was furnace-cooled to room temperature in flowing ammonia, and then passivated in a 60 ml/min flow of 1 mol% O_2/He for 3 h prior to air exposure.

Co_3Mo_3C/Al_2O_3 catalysts were prepared from freshly prepared Co_3Mo_3N/Al_2O_3 catalysts which were not passivated. Following furnace cooling in flowing ammonia (60 ml/min), a Co_3Mo_3N/Al_2O_3 catalyst was degassed for 30 min in 60 ml/min He at 295 K. Under continued He flow (60 ml/min), the catalyst sample was heated to 673 K over 10 min, the flow switched to 60 ml/min of a 20 mol% CH_4/H_2 mixture (Airgas) and the sample temperature increased from 673 to 950 K at a rate of 0.5 K/min. The flow was then switched to 60 ml/min He and the Co_3Mo_3C/Al_2O_3 catalyst was furnace-cooled to room temperature. The Co_3Mo_3C/Al_2O_3 catalyst was passivated in a 60 ml/min flow of 1 mol% O_2/He for 3 h at room temperature prior to air exposure.

2.2. Catalyst characterization

2.2.1. *XRD measurements*

XRD patterns were acquired on a Rigaku Geigerflex powder diffractometer outfitted with a Cu Kα

source ($\lambda = 1.5418$ Å), and is interfaced to a personal computer for data acquisition and analysis using Materials Data Incorporated (MDI) DataScan and Jade Plus 5.0 software. Catalysts which were subjected to a sulfidation pretreatment prior to XRD analysis were heated over 1 h from room temperature to a maximum temperature in the range of 623–1023 K in a 60 ml/min flow of a 3.0 mol% H_2S/H_2 mixture and holding at the maximum temperature for 2 h. The catalysts were then cooled to room temperature and the gas flow switched to 45 ml/min of He for 15 min. Finally, the catalyst samples were passivated in a flow of a 1 mol% O_2/He mixture as described above prior to mounting in the X-ray diffractometer. The maximum sulfidation temperatures employed are those listed in the figures.

2.2.2. BET and pulsed chemisorption measurements

Single point BET surface area measurements were obtained using a Micromeritics PulseChemisorb 2700 apparatus. Catalyst samples (~0.10 g) were placed in a quartz U-tube, degassed in a 60 ml/min flow of He for 30 min at room temperature, followed by a 2 h degassing in a 45 ml/min flow of He at 623 K, then cooled to room temperature under flowing He. The BET measurements were carried out following a procedure described elsewhere [5].

CO pulsed chemisorption measurements were also carried out using the Micromeritics PulseChemisorb 2700 instrument. Chemisorption capacity measurements were conducted using CO (Airco, 99.999% pure) as the probe gas. Catalyst samples (~0.10 g) were degassed in a 60 ml/min flow of He at room temperature for 2 h and were then sulfided in situ by heating over 1 h from room temperature to the sulfidation temperature in a 60 ml/min flow of 3 mol% H_2S/H_2 mixture. The samples were held at the sulfidation temperature for 2 h in the flowing H_2S/H_2 mixture. The sulfided samples were then reduced in a 60 ml/min flow of H_2 for 1 h at the sulfidation temperature or 623 K, which ever temperature was lower. Finally, all samples were degassed in 60 ml/min He at 673 K for 1 h. The CO chemisorption measurements were carried out at 273 K following a procedure reported previously [5]. The units of the reported chemisorption capacities are micromoles of CO per gram of catalyst (μmol/g).

2.2.3. Infrared spectroscopy measurements

Infrared (IR) spectroscopic measurements were carried out in the transmission mode using a Mattson RS-1 FT-IR spectrometer equipped with a narrow-band MCT detector. Catalyst samples were mounted in a bakeable, stainless steel ultrahigh vacuum (UHV) chamber equipped with a high pressure cell that can be isolated from the vacuum chamber. The system has been described in detail elsewhere [27]. Approximately 5.0 mg of catalyst was pressed at ~10,000 psi into a nickel metal mesh (50×50 mesh size, 0.002 in. wire diameter); the area of the pressed samples was 0.80 cm^2. The temperature of the sample was monitored by means of a chromel–alumel thermocouple spot-welded to the nickel mesh. Following mounting in the UHV system, samples of the Co–MoO_3/Al_2O_3 and Co–Mo_2C/Al_2O_3 catalysts were evacuated to 10^{-3} Torr (1 Torr = 133.3 Pa) over a period of ~30 min, and were then subjected to consecutive sulfidation treatments which consisted of heating to 623 K in 100 Torr of a 3.03% H_2S/H_2 mixture for 30 min. Following sulfidation, the catalyst samples were reduced in a 60 ml/min flow of H_2 at 623 K for 1 h. The high pressure cell was then evacuated and the catalyst sample flashed to 673 K in UHV and then cooled to room temperature. The typical system base pressure following such a procedure was $\sim 5.0 \times 10^{-9}$ Torr. Catalyst samples were exposed to 5.0 Torr of CO at 298 K and an IR spectrum was acquired (32 scans, 4 cm^{-1}). IR spectra are reproduced without any smoothing treatment, being prepared by subtracting the IR spectrum acquired immediately prior to dosing from the IR spectrum acquired after dosing.

2.2.4. Thiophene HDS activity measurements

Thiophene HDS activity measurements were carried out using an atmospheric pressure flow reactor that has been described in detail elsewhere [5]. Activity measurements were carried out at a reaction temperature of 643 K using a reactor feed consisting of a 3.2 mol% thiophene/H_2 mixture.

Prior to the measurement of thiophene HDS activities, catalysts were subjected to one of three different pretreatments: (1) degas in He (60 ml/min) at room temperature for 30 min; (2) reduction in H_2 by heating the catalyst sample from room temperature to 650 K (5.9 K/min) in a 60 ml/min flow of H_2 and holding at 650 K for 2 h; (3) sulfidation by heating from room

temperature to the sulfidation temperature in 1 h in a 60 ml/min flow of 3 mol% H_2S/H_2 and holding at the sulfidation temperature for 2 h. Following pretreatment, the gas flow was switched to a 60 ml/min flow of He, the temperature was adjusted to the reaction temperature of 643 K, and the flow was switched to the 3.2 mol% thiophene/H_2 reactor feed (50 ml/min). The reaction was carried out for 24 h, with automated sampling of the gas effluent occurring at 1 h intervals. Thiophene HDS activities are reported in units of nanomoles of thiophene converted to products per gram of catalyst per second (nmol Th/g cat s) and were calculated from the total product peak areas calculated from the chromatogram after 24 h of reaction time.

3. Results and discussion

The over-arching theme to HDS studies of alumina-supported carbide and nitride catalysts in our laboratory has been to compare them directly to conventional sulfide-based catalysts of similar metal composition. The comparison sulfide catalysts are prepared from the same oxidic precursors used to synthesize the carbide or nitride catalysts. As a result, the naming scheme adopted in this article for the sulfide catalysts indicates the parent oxidic precursor from which they (and the carbide or nitride catalyst under comparison) were made. Thus, Co–Mo_2C/Al_2O_3 catalysts are compared with sulfided Co–MoO_3/Al_2O_3 catalysts while Co_3Mo_3C/Al_2O_3 catalysts are compared with sulfided $CoMoO_4/Al_2O_3$ catalysts, reflecting that the comparison sulfide catalysts are made from different oxidic precursors. This is an important distinction as the method of preparation of the oxidic precursor can influence the HDS catalytic properties of the resulting sulfide catalyst [1].

3.1. Catalyst synthesis and catalyst characterization

While γ-Al_2O_3 has been most frequently used to support metal carbide and nitride phases, syntheses have also been described for the preparation of β-Mo_2C supported on silica (SiO_2) [28,29], zirconia (ZrO_2) [30], a zeolite (ZSM-5) [31,32], and carbon [33,34], for α-MoC_{1-x} ($x \approx 0.5$) supported on a zeolite (ZSM-5) [32], and for γ-Mo_2N supported on titania (TiO_2) [35] and carbon [36]. The syntheses carried out in our laboratory of alumina-supported β-Mo_2C, MoC_{1-x} ($x \approx 0.5$), and γ-Mo_2N are similar to those utilized by others and will be described briefly here [5,7]. Each synthesis utilizes alumina-supported molybdenum trioxide precursors (MoO_3/Al_2O_3) prepared by impregnation of γ-Al_2O_3 with ammonium heptamolybdate followed by drying and calcination at 773 K. The TPR method is used to convert the oxidic precursors to the desired alumina-supported carbide or nitride phase. Mo_2C/Al_2O_3 catalysts are prepared by carburization of the oxidic precursors in a flowing 20 mol% CH_4/H_2 mixture while heating to a maximum temperature of 950–970 K; Mo_2N/Al_2O_3 catalysts are synthesized by nitridation of the oxidic precursors in flowing NH_3 while heating to 970 K. Finally, MoC_{1-x}/Al_2O_3 catalysts are prepared in a two-step synthesis in which MoO_3/Al_2O_3 precursors are initially nitrided in flowing NH_3 to give alumina-supported γ-Mo_2N, followed by carburization in a flowing 20 mol% CH_4/H_2 mixture to give alumina-supported MoC_{1-x} ($x \approx 0.5$). The supported carbide and nitride phases are pyrophoric, and the catalysts must be passivated following synthesis; this is most often accomplished by flowing diluted oxygen (e.g. 1 mol% O_2/He, 298 K, 2 h) over the catalysts prior to air exposure. For sufficiently high loadings, alumina-supported β-Mo_2C, MoC_{1-x} ($x \approx 0.5$), and γ-Mo_2N can be identified using XRD and average crystallite sizes can be calculated using the Scherrer equation [37] and the full width at half maximum (FWHM) of prominent diffraction peaks [7]. Care must be taken when preparing supported Mo carbides to avoid the deposition of polymeric carbon on the catalyst surface during TPR [38,39], and to achieve maximum replacement of N with C in the synthesis of MoC_{1-x}/Al_2O_3 catalysts from Mo_2N/Al_2O_3 intermediate products [39].

In addition to XRD, alumina-supported Mo carbide and nitride catalysts have been characterized by a variety of other techniques including transmission electron microscopy (TEM) [38], temperature programmed desorption (TPD) [5,38,40], IR spectroscopy [5,11,41–43] and X-ray photoelectron spectroscopy (XPS) [23,39,44,45]. Instead of summarizing the results of these characterization studies here, those most pertinent to the HDS catalytic properties will be discussed in the following section of this article.

The syntheses of Co–Mo_2N/Al_2O_3 [24,46] and of Co–Mo_2C/Al_2O_3 [46] catalysts were outlined previously, and the preparation of a series of Co–Mo_2C/Al_2O_3 catalysts is described in the current study. The Co-promoted Mo carbide and nitride catalysts were prepared very simply by impregnation of Mo_2C/Al_2O_3 and Mo_2N/Al_2O_3 catalysts with aqueous solutions of cobalt nitrate followed by drying. To minimize the decomposition of the supported carbide and nitride phases, the impregnated catalysts were dried under vacuum at room temperature and then passivated under a static 1 mol% O_2/He mixture. If the Co–Mo_2C/Al_2O_3 and Co–Mo_2N/Al_2O_3 catalysts were exposed directly to air following vacuum drying, a significant amount of heat was liberated and the color of the catalysts lightened considerably. Together, these observations suggest that passivation of the promoted catalysts is necessary to avoid deep oxidation of the supported Co–Mo_2C and Co–Mo_2N particles upon exposure to air. To our knowledge, the only characterization of Co-promoted Mo_2C/Al_2O_3 and Mo_2N/Al_2O_3 catalysts reported in the literature has been the results of chemisorption measurements [24,46].

A number of laboratories have reported the synthesis of alumina-supported bimetallic nitrides (Co–Mo–N, Ni–Mo–N) [23–26,47–50], although phase pure materials were prepared in only one case [26]. The incorrect identification of unsupported Ni–Mo–N phases in the literature [51,52] most likely contributed to the preparation of impure alumina-supported Ni–Mo–N catalysts in two cases [48,50]. Bimetallic nitrides initially identified to be pure Ni_3Mo_3N [51,52] were later determined to be impure materials in which Ni_2Mo_3N was the major phase [53,54]. It was subsequently shown that pure Ni_2Mo_3N can be prepared by nitridation of metallorganic hydroxide [54] or bimetallic oxide [55,56] precursors in flowing NH_3. Ni–Mo–N/Al_2O_3 catalysts in which the major nitride phase was erroneously identified to be Ni_3Mo_3N were prepared from oxidic precursors with Ni/Mo = 1.0. In addition to "Ni_3Mo_3N", Chu et al. [48] noted the presence of a substantial Ni impurity in their catalyst while the XRD pattern of the catalyst prepared by Yuhong et al. [50] shows a substantial γ-Mo_2N impurity. Others have reported syntheses of Ni–Mo–N/Al_2O_3 catalysts but no bimetallic nitride phases were identified [23,49].

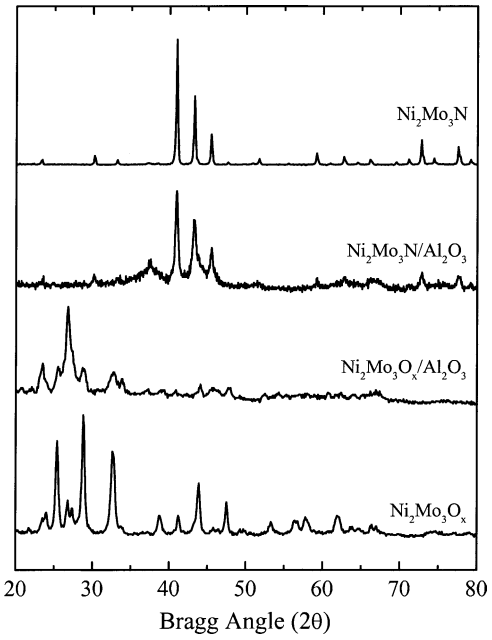

Fig. 1. XRD patterns for $Ni_2Mo_3O_x$, $Ni_2Mo_3O_x/Al_2O_3$, Ni_2Mo_3N/Al_2O_3, and Ni_2Mo_3N. The theoretical loading of the supported oxide precursor and bimetallic nitride is 50 wt.% Ni_2Mo_3N. Reproduced with permission from Chem. Mater. 14 (2002) 4049–4058; Copyright 2002 Am. Chem. Soc.

We have recently described the synthesis of phase pure, alumina-supported Ni_2Mo_3N catalysts [26]. Shown in Fig. 1 are the XRD patterns for bulk and alumina-supported oxidic precursors ($Ni_2Mo_3O_x$ and $Ni_2Mo_3O_x/Al_2O_3$, respectively) having the appropriate metal stoichiometry (Ni/Mo = 0.67), and for samples of these oxidic materials that were nitrided in flowing NH_3 to a maximum TPR temperature of 1173 K. The XRD patterns for unsupported Ni_2Mo_3N and for a 50 wt.% Ni_2Mo_3N/Al_2O_3 catalyst are consistent with those reported by others for phase pure Ni_2Mo_3N [54,55]. By varying the total metal loading in the oxidic precursors, a series of Ni_2Mo_3N/Al_2O_3 catalysts were prepared for which the XRD patterns shown in Fig. 2 indicate that alumina-supported Ni_2Mo_3N catalysts can be prepared with a range of crystallite sizes. For the 30 wt.% Ni_2Mo_3N/Al_2O_3 catalyst, an average crystallite size of 16 nm can be calculated using the Scherrer equation and the FWHM of the peak at 40.9°. The presence of Ni_2Mo_3N on the alumina support is inferred for loadings below 20 wt.% Ni_2Mo_3N, with the assumption that the

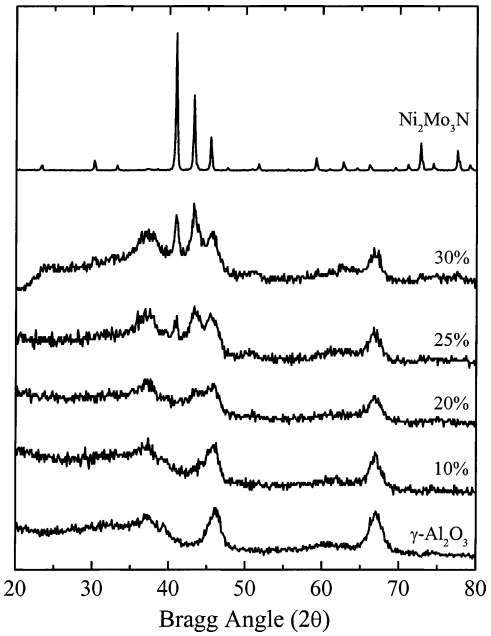

Fig. 2. XRD patterns for Ni_2Mo_3N/Al_2O_3 catalysts with theoretical loadings of 10, 20, 25, and 30 wt.% Ni_2Mo_3N. Also shown for comparison purposes, are the XRD patterns for γ-Al_2O_3 and Ni_2Mo_3N. Reproduced with permission from Chem. Mater. 14 (2002) 4049–4058; Copyright 2002 Am. Chem. Soc.

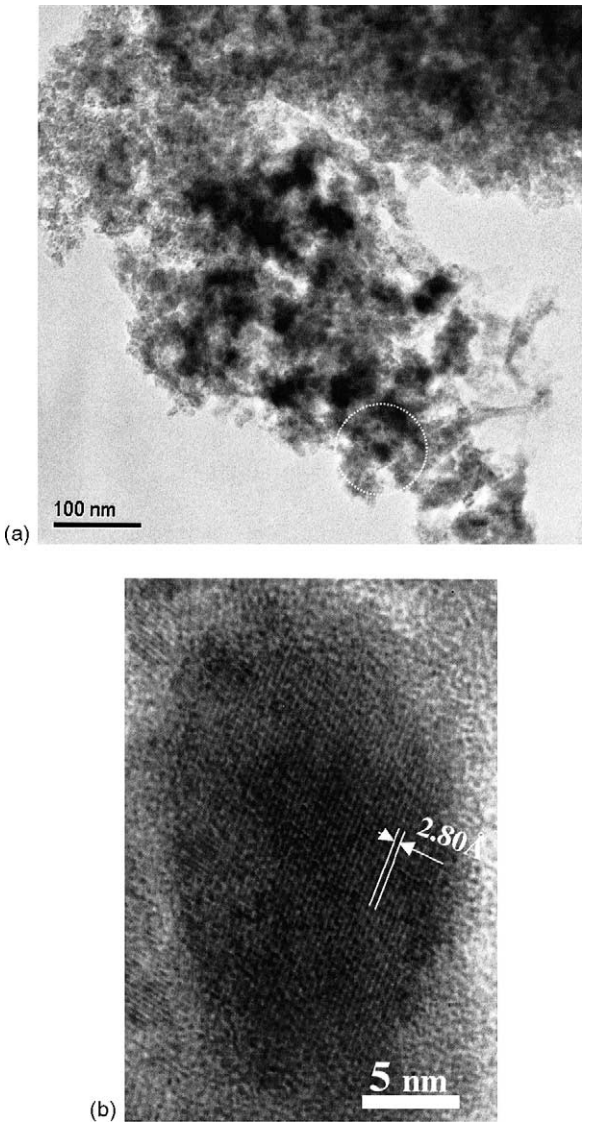

Fig. 3. TEM micrographs of a 30 wt.% Ni_2Mo_3N/Al_2O_3 catalyst. Reproduced with permission from Chem. Mater. 14 (2002) 4049–4058; Copyright 2002 Am. Chem. Soc.

crystallite size is below the detection limit for XRD. TEM investigation of a 30 wt.% Ni_2Mo_3N/Al_2O_3 catalyst reveals a range of Ni_2Mo_3N particle sizes (see Fig. 3a), but no evidence for crystalline impurities. Fig. 3b shows an oval-shaped Ni_2Mo_3N particle on the alumina support having dimensions of 15 nm × 21 nm.

Syntheses of nitrided Co–Mo/Al_2O_3 catalysts [23–26,57] have been described in the literature, but in only one case was the preparation of phase pure, alumina-supported Co_3Mo_3N reported [26]. In this last case, a series of Co_3Mo_3N/Al_2O_3 catalysts were prepared by nitridation of $CoMoO_4/Al_2O_3$ precursors in flowing NH_3 to a maximum temperature of 1023 K. The synthesis of Co_3Mo_3C/Al_2O_3 catalysts has also recently been described [26]. Attempts to prepare alumina-supported Co_3Mo_3C by carburization of $CoMoO_4/Al_2O_3$ precursors were unsuccessful, yielding Co metal and β-Mo_2C on the alumina support [26]. Instead, Co_3Mo_3C/Al_2O_3 catalysts were prepared in a two-step synthesis in which $CoMoO_4/Al_2O_3$ precursors were first nitrided in flowing NH_3 to give Co_3Mo_3N/Al_2O_3 intermediate products that were subsequently carburized in a flowing 20 mol% CH_4/H_2 mixture to a maximum temperature of 950 K. XRD patterns and TEM images are consistent with the successful synthesis of alumina-supported Co_3Mo_3C, but elemental analysis of a 22.5 wt.% Co_3Mo_3C/Al_2O_3 catalyst suggested incomplete replacement of N with

C resulting in a supported bimetallic phase of composition $Co_{3.00}Mo_{3.00}C_{0.66}N_{0.31}$ [26].

In addition to the characterization studies described above, alumina-supported bimetallic carbide and nitride catalysts have been characterized by IR spectroscopy [57] and XPS [23]. In their IR spectroscopic studies of nitrided Co–Mo/Al_2O_3 catalysts, Li and coworkers [57] used both CO and NO as probe molecules. Consistent with IR spectroscopic studies of conventional sulfide catalysts, NO was observed to adsorb more strongly on the nitrided Co–Mo/Al_2O_3 catalysts than did CO, and ν_{NO} absorbances could be assigned to Mo and Co sites.

3.2. HDS catalytic properties

As mentioned in Section 1, alumina-supported β-Mo_2C and γ-Mo_2N catalysts have been observed to be more active than sulfided Mo/Al_2O_3 catalysts for the HDS of thiophene and other organosulfur compounds [5–7,10–12]. The HDS properties of alumina-supported α-MoC_{1-x} ($x \approx 0.5$) catalysts have been less thoroughly investigated. In our laboratory, thiophene HDS activities were measured for Mo_2N/Al_2O_3, MoC_{1-x}/Al_2O_3 and Mo_2C/Al_2O_3 catalysts having loadings in the range of 1.5–20 wt.% Mo [7]. The relative HDS activities of these catalysts, averaged over all loadings, are shown in Fig. 4. When supported on alumina, β-Mo_2C and γ-Mo_2N are 41 and 22% more active for thiophene HDS, respectively, than sulfided MoO_3/Al_2O_3 catalysts with similar Mo loadings, while the HDS activities of alumina-supported α-MoC_{1-x} ($x \approx 0.5$) catalysts are similar to those of the sulfided Mo catalysts.

Review of the literature reveals the most commonly used pretreatment for Mo carbide and nitride catalysts to be reduction in flowing H_2. In the thiophene HDS studies described above, for example, McCrea et al. [7] utilized a reduction pretreatment (60 ml/min H_2, 750 K, 2 h) prior to bringing alumina-supported β-Mo_2C, MoC_{1-x} ($x \approx 0.5$) and γ-Mo_2N catalysts on-stream. The purpose of a reduction pretreatment is to remove the thin, passive oxide layer formed on the Mo carbide and nitride particles following synthesis, hopefully exposing oxygen-free surfaces to the reactor feed. IR spectroscopic studies suggest otherwise, however. As shown at the bottom of Fig. 5, the IR spectrum of adsorbed CO on a freshly reduced 10 wt.% Mo_2C/Al_2O_3 catalyst reveals the most prominent ν_{CO} absorbance to be at 2170 cm^{-1}, which can be assigned to CO adsorbed to coordinately unsaturated (cus) Mo^{4+} sites on the catalyst surface. The high oxidation state of these Mo sites suggests that a reduction pretreatment at 750 K does not fully remove the passive oxide layer on the supported β-Mo_2C particles. Similar results were reported by Li and coworkers [41,42] for Mo_2N/Al_2O_3 catalysts; IR spectra of adsorbed CO on a catalyst subjected to a reduction pretreatment at 873 K showed a large ν_{CO} absorbance at 2179 cm^{-1}. While these researchers show that higher reduction temperatures yield Mo_2N/Al_2O_3 catalysts with higher CO chemisorption capacities, it is not clear to what extent high temperature H_2 reduction causes the removal of N from the supported nitride particles. The passive oxide layer on the Mo_2N/Al_2O_3 catalysts was more effectively removed by re-nitridation of the catalysts at 723–873 K [42].

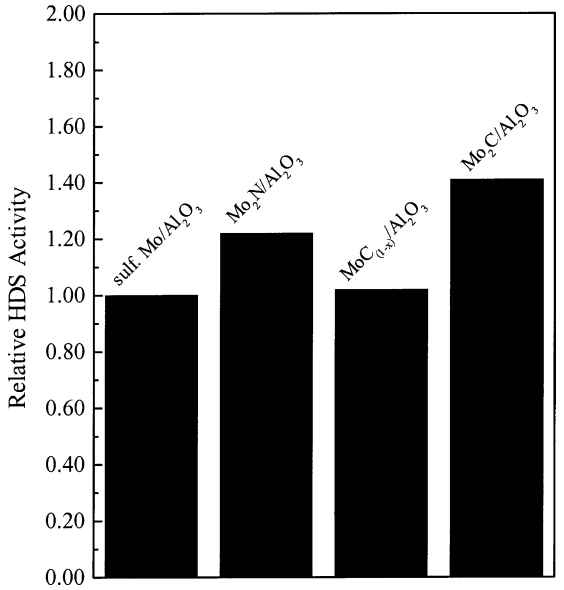

Fig. 4. Relative HDS activities of Mo_2N/Al_2O_3, MoC_{1-x}/Al_2O_3, Mo_2C/Al_2O_3 and sulfided Mo/Al_2O_3 catalysts having loadings in the range of 1.5–20 wt.% Mo [7].

With the knowledge that alumina-supported Mo carbide and nitride catalysts expose oxidized Mo species following a H_2 reduction pretreatment at temperatures as high as 873 K, it is of interest to probe the stability of these cus Mo sites under the sulfiding

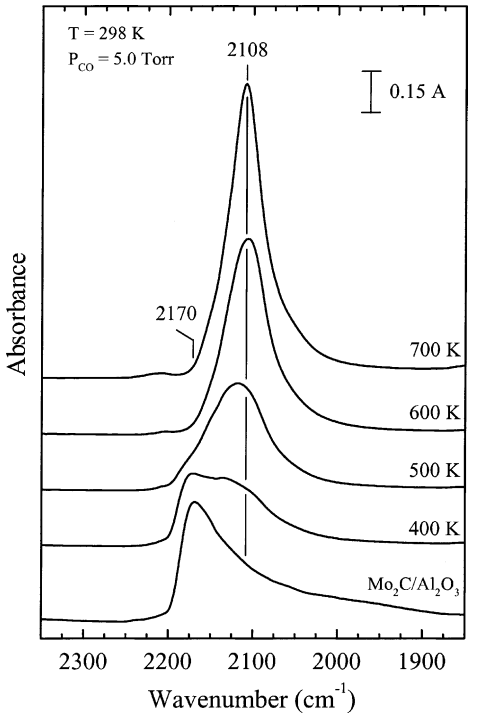

Fig. 5. IR spectra of adsorbed CO on a freshly reduced 10 wt.% Mo_2C/Al_2O_3 catalyst and the same catalyst treated in a thiophene/H_2 mixture ($P_{Th} = 5.0$ Torr, $P_{H_2} = 750$ Torr) at the given temperatures for 1 h. Following the thiophene H_2 treatments, the catalyst was outgassed in UHV at 750 K prior to CO adsorption at 298 K. Reprinted with permission from J. Catal. 164 (1996) 109–121; Copyright 1996 Elsevier.

conditions present in an HDS reactor. As shown in Fig. 5, IR spectra of adsorbed CO on a 10 wt.% Mo_2C/Al_2O_3 catalyst heated in a thiophene/H_2 mixture ($P_{C_4H_4S} = 5.0$ Torr, $P_{H_2} = 750$ Torr) to increasing temperatures for 1 h periods reveal substantial changes in the adsorption sites at the surface of a 10 wt.% Mo_2C/Al_2O_3 catalyst [5]. As the temperature of the thiophene/H_2 treatments increases, a strong ν_{CO} absorbance develops at 2108 cm^{-1} that is indistinguishable from that observed for CO adsorbed on a conventional sulfided MoO_3/Al_2O_3 catalyst. Similar results were obtained for a 10 wt.% Mo_2N/Al_2O_3 catalyst [5]. XRD patterns of fresh and tested 30 wt.% Mo_2C/Al_2O_3 and Mo_2N/Al_2O_3 catalysts (1.8 mol% thiophene/H_2, 693 K, 24 h) on the other hand, were found to be nearly identical [5], indicating that the bulk structure of the supported β-Mo_2C and γ-Mo_2N

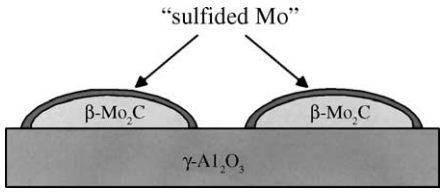

Fig. 6. A schematic representation of a Mo_2C/Al_2O_3 catalyst during thiophene HDS. Reprinted with permission from J. Catal. 164 (1996) 109–121; Copyright 1996 Elsevier.

particles remained unchanged. Taken together, the IR spectroscopic and XRD results led us to propose a model for the active surfaces of Mo_2C/Al_2O_3 (and Mo_2N/Al_2O_3) catalysts that is shown schematically in Fig. 6. In this model, β-Mo_2C and γ-Mo_2N particles serve as supports on which a thin layer of sulfided Mo forms under HDS conditions. We describe this thin layer as "sulfided Mo" on the basis that its ν_{CO} absorbance is indistinguishable from that observed for a conventional sulfided MoO_3/Al_2O_3 catalyst. It is possible that this surface phase contains significant amounts of carbon and should more accurately be described as a carbosulfide phase as proposed by Oyama and coworkers [9] for HDS over unsupported β-Mo_2C. The key point is that this surface phase has a higher HDS activity than does a conventional sulfided Mo catalyst. Combining the properties of high melting point, hardness and strength [15,17], the molybdenum carbide and nitride particles serve as rigid substrates in our model for a sulfided Mo phase exposing large numbers of cus Mo sites on which thiophene adsorption and reaction occurs. CO and O_2 chemisorption measurements and thiophene HDS turnover frequencies (TOFs) are consistent with this model [7]. Mo_2C/Al_2O_3 and Mo_2N/Al_2O_3 catalysts sulfided at 623 K had higher chemisorption capacities than sulfided MoO_3/Al_2O_3 catalysts with similar Mo loadings, but the carbide, nitride and sulfide catalysts were observed to have nearly identical TOFs [5,7]. As a result, we concluded that the higher HDS activities of Mo_2C/Al_2O_3 and Mo_2N/Al_2O_3 catalysts can be traced to higher active site densities, and not more active sites. It is worth noting that this conclusion does not invoke "platinum-like" behavior (as described in Section 1) to explain the high HDS activity of Mo_2C/Al_2O_3 and Mo_2N/Al_2O_3 catalysts. "Platinum-like" sites on the Mo carbide and nitride catalysts would be expected

to have high thiophene HDS TOFs; instead, the Mo_2C/Al_2O_3 and Mo_2N/Al_2O_3 catalysts have TOFs similar to that of sulfided MoO_3/Al_2O_3 catalysts. In contrast, we have measured a significantly higher TOF for highly active sulfided Rh/Al_2O_3 catalysts under similar reaction conditions [58].

In order to further access the effect of sulfidation on the HDS properties of Mo_2C/Al_2O_3 catalysts, XRD and pulsed CO chemisorption have been used to probe the bulk structure and adsorption site densities, respectively, of Mo_2C/Al_2O_3 catalysts subjected to pretreatment in a flowing 3.0 mol% H_2S/H_2 mixture at increasing temperatures. Shown in Fig. 7 are the XRD patterns for a freshly prepared, 50 wt.% Mo_2C/Al_2O_3 catalyst as well as samples of this catalyst subjected to sulfidation pretreatments (3.0 mol% H_2S/H_2, 2 h) at the listed temperatures. The XRD pattern for the freshly prepared Mo_2C/Al_2O_3 catalyst is in good agreement with a reference pattern for β-Mo_2C (card no. 35-787 [59]). For sulfidation temperatures up to 723 K, at the upper end of the temperature range for HDS processing [1], there is little change in the XRD patterns of the Mo_2C/Al_2O_3 catalyst. For sulfidation temperatures of 823 K or higher, however, reflections

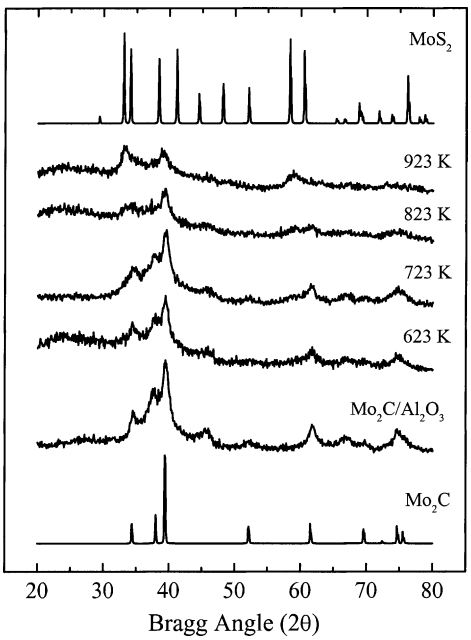

Fig. 7. XRD patterns of 50 wt.% Mo_2C/Al_2O_3 catalysts subjected to sulfidation pretreatments at the listed temperatures.

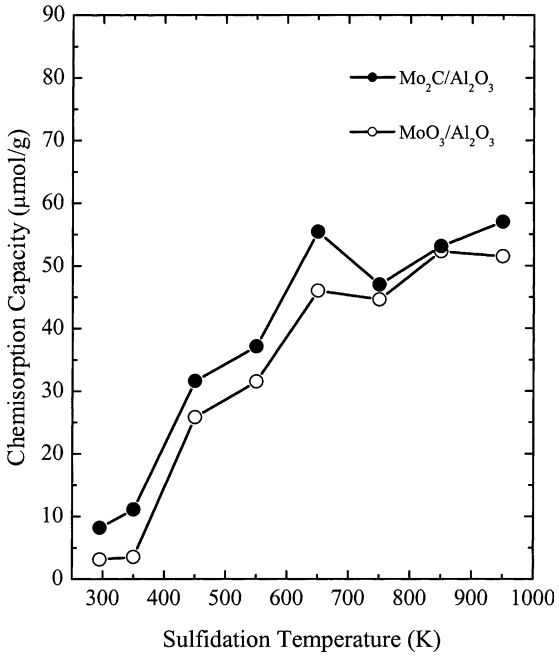

Fig. 8. CO chemisorption capacities for Mo_2C/Al_2O_3 (16 wt.% Mo_2C) and MoO_3/Al_2O_3 (21 wt.% MoO_3) catalysts as a function of the sulfidation pretreatment temperature.

become apparent that are consistent with those in a reference pattern for MoS_2 (card no. 17-0744 [59]). Plotted in Fig. 8 are the CO chemisorption capacities of Mo_2C/Al_2O_3 and MoO_3/Al_2O_3 catalysts having similar Mo loadings (16 wt.% Mo_2C and 21 wt.% MoO_3, respectively) that have been sulfided at the indicated temperatures. Consistent with chemisorption results published previously for Mo_2C/Al_2O_3 and MoO_3/Al_2O_3 catalysts having a wide range of loadings and sulfided at 623 K [7], the Mo_2C/Al_2O_3 catalysts have consistently higher CO chemisorption capacities over the entire range of sulfidation temperatures than do MoO_3/Al_2O_3 catalysts having the same Mo loading. These results indicate that the sulfided Mo layer formed at the surface of alumina-supported β-Mo_2C particles maintains a higher site density than for sulfided MoO_3/Al_2O_3 catalysts, although the difference narrows for sulfidation temperatures of 723 K and above where MoS_2 crystallites are detected on the Mo_2C/Al_2O_3 catalysts via XRD (see Fig. 7).

The HDS activity data plotted in Fig. 9 clearly show that a 16 wt.% Mo_2C/Al_2O_3 catalyst is more

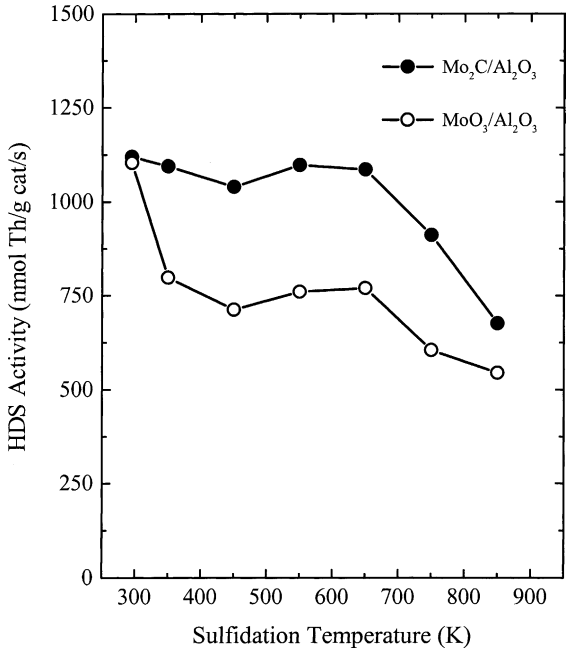

Fig. 9. Thiophene HDS activities for Mo_2C/Al_2O_3 (16 wt.% Mo_2C) and MoO_3/Al_2O_3 (21 wt.% MoO_3) catalysts as a function of the sulfidation temperature.

active than a sulfided MoO_3/Al_2O_3 catalyst (21 wt.% MoO_3) over the entire range of sulfidation temperatures. For typical sulfidation temperatures of 550–650 K, the 16 wt.% Mo_2C/Al_2O_3 catalyst is 43% more active for thiophene HDS than the MoO_3/Al_2O_3 catalyst (21 wt.% MoO_3). For sulfiding temperatures of 750–850 K, the HDS activity of the Mo_2C/Al_2O_3 catalyst declines, but remains 38% higher than that of the sulfided MoO_3/Al_2O_3 catalyst. These results suggest that Mo_2C/Al_2O_3 catalysts have excellent resistance to deep sulfidation, as indicated by their high HDS activities (relative to sulfided MoO_3/Al_2O_3 catalysts) despite sulfidation pretreatments at high temperatures. Previous research in our laboratory showed that the CO and O_2 chemisorption capacities of Mo_2C/Al_2O_3 and MoO_3/Al_2O_3 catalysts (sulfided at 623 K) correlate well with their thiophene HDS activities for catalysts with a wide range of loadings [5,7]. As described above, the Mo_2C/Al_2O_3 and MoO_3/Al_2O_3 catalysts were observed to have similar TOFs and the higher HDS activities of the carbide catalysts (relative to the sulfided MoO_3/Al_2O_3 catalysts) were traced to higher site densities. The data presented in Figs. 8 and 9 are qualitatively consistent with this observation as the HDS activities and CO chemisorption capacities of a 16 wt.% Mo_2C/Al_2O_3 catalyst sulfided at a range of temperatures are uniformly higher than those of a MoO_3/Al_2O_3 catalyst having a similar Mo loading (21 wt.% MoO_3). Focusing on sulfidation temperatures of 550–650 K, the 16 wt.% Mo_2C/Al_2O_3 catalyst has thiophene HDS activities and CO chemisorption capacities that are 43 and 20% higher, respectively, than those for the sulfided MoO_3/Al_2O_3 catalyst.

Given that the sites on Mo_2C/Al_2O_3 catalysts are similar to those on sulfided MoO_3/Al_2O_3 catalysts under HDS reaction conditions, a logical next step is to explore the possibility of promoting the HDS activities of Mo_2C/Al_2O_3 (and Mo_2N/Al_2O_3) catalysts via the addition of a second metal. The addition of a promoting metal (Co, Ni) to molybdenum-based hydrotreating catalysts has long been known to increase the activity of these materials for removal of heteroatoms from impurities in fossil fuel feedstocks [1]. The optimal Co/Mo molar ratio typically lies in the range of 0.3–0.5, and the added Co increases the HDS activity by as much as 10-fold relative to the unpromoted sulfided Mo catalyst. Typical metal loadings in commercial Co–Mo/Al_2O_3 catalysts are reported to be in the range of 1–4 wt.% Co and 8–16 wt.% Mo [1].

To our knowledge, only two preliminary studies have appeared in the literature in which the Co promotion of Mo_2C/Al_2O_3 and Mo_2N/Al_2O_3 catalysts has been investigated [24,46]. In both cases, significant increases in the thiophene HDS activities of the Mo carbide and nitride catalysts were observed upon Co promotion. With the goal of further exploring the potential of molybdenum carbide catalysts for use in HDS processing, we have investigated the effects of Co promotion on the thiophene HDS activity of Mo_2C/Al_2O_3 catalysts in greater detail. In doing so, we have compared the Co–Mo_2C/Al_2O_3 catalysts with sulfided Co–MoO_3/Al_2O_3 catalysts prepared from the same oxidic precursors (MoO_3/Al_2O_3) used to prepare the carbide catalysts. Since the highest HDS activity for Mo_2C/Al_2O_3 catalysts was previously observed for a Mo_2C loading of 16 wt.% [7], the Co promotion studies of Mo_2C/Al_2O_3 catalysts were carried out for catalysts with this loading. At each Co/Mo molar ratio investigated, the Co–Mo_2C/Al_2O_3

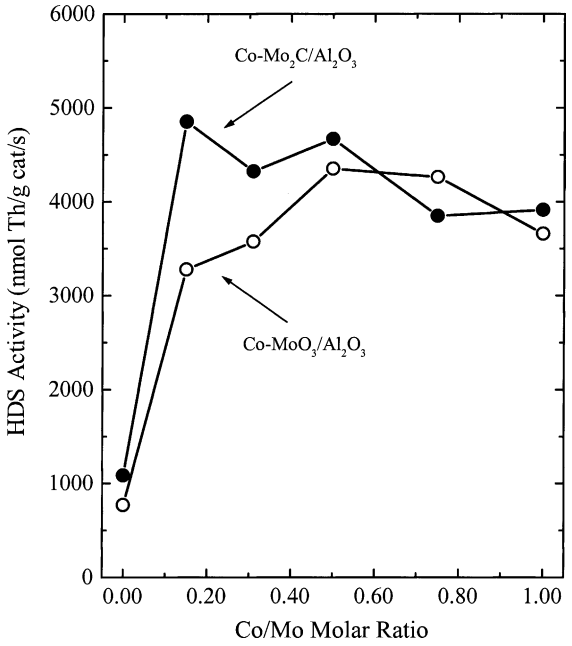

Fig. 10. Thiophene HDS activities for Co-promoted Mo_2C/Al_2O_3 and MoO_3/Al_2O_3 catalysts as a function of the Co/Mo ratio.

catalysts were compared to sulfided $Co–MoO_3/Al_2O_3$ catalysts with similar metal loadings. Both sets of catalysts were pretreated similarly—sulfidation in flowing 3.0 mol% H_2S/H_2 for 2 h at 650 K. Focusing initially on the sulfided $Co–MoO_3/Al_2O_3$ catalysts, the addition of Co strongly enhances the thiophene HDS activity of the catalysts, with the activity increased by a factor of 5.7 for an optimal Co/Mo mole ratio of 0.50 (see Fig. 10), which is consistent with the results reported by others [1]. The magnitude of the HDS activity increase and the optimal Co/Mo ratio for sulfided Co–Mo catalysts are sensitive to a number of factors, including the catalyst preparation method and the pretreatment utilized [1]. In this research, neither the $Co–MoO_3/Al_2O_3$ nor the $Co–Mo_2C/Al_2O_3$ catalysts were calcined following addition of the cobalt promoter as calcination would result in oxidation of the alumina-supported β-Mo_2C. It was deemed important to maintain a consistent procedure for promoting both the $Co–MoO_3/Al_2O_3$ and $Co–Mo_2C/Al_2O_3$ catalysts, so none of the catalysts were calcined following addition of the Co promoter.

In our previous studies of $Co–Mo_2N/Al_2O_3$ catalysts, it was found that the HDS activity exhibited a strong dependence upon the pretreatment used [24], with a catalyst subjected to a sulfidation pretreatment (3.0 mol% H_2S/H_2, 623 K, 2 h) observed to be nearly 60% more active than a sample of the same catalyst pretreated in hydrogen (H_2, 750 K, 2 h). Similar results were obtained for the $Co–Mo_2C/Al_2O_3$ catalysts in the current study and, as a result, the HDS activities reported are for catalysts subjected to a sulfidation pretreatment (3.0 mol% H_2S/H_2, 650 K, 2 h) unless otherwise specified. As shown in Fig. 10, the trend in HDS activity for the $Co–Mo_2C/Al_2O_3$ catalysts as a function of the Co/Mo molar ratio is similar to that observed for the sulfided $Co–MoO_3/Al_2O_3$ catalysts except for two important differences. For the $Co–Mo_2C/Al_2O_3$ catalysts, the optimal Co/Mo ratio is lower (0.15 vs. 0.50 for the sulfided $Co–MoO_3/Al_2O_3$ catalysts) and the maximum HDS activity is 12% higher than that of the most active sulfided $Co–MoO_3/Al_2O_3$ catalyst (Co/Mo = 0.50). The HDS activity of the $Co–Mo_2C/Al_2O_3$ catalyst with Co/Mo = 0.15 is 4.5 times higher than that of the unpromoted Mo_2C/Al_2O_3 catalyst, and is 48% higher than the sulfided $Co–MoO_3/Al_2O_3$ catalyst with the same Co/Mo molar ratio. Based on these results, less Co is needed to achieve optimal promotion of the $Co–Mo_2C/Al_2O_3$ catalysts relative to the sulfided $Co–MoO_3/Al_2O_3$ catalysts. Shown in Fig. 11 are IR spectra in the ν_{CO} region for $Co–Mo_2C/Al_2O_3$ and $Co–MoO_3/Al_2O_3$ catalysts (Co/Mo = 0.15) sulfided at 623 K and then reduced in flowing H_2 at 623 K before exposing them to 5.0 Torr CO. Starting with the sulfided $Co–MoO_3/Al_2O_3$ catalyst, two ν_{CO} absorbances are apparent at 2105 and 2062 cm^{-1}. The peak positions are similar to and the peak intensities are consistent with those reported by Bachelier et al. [60] and Maugé and Lavalley [61] for CO adsorbed on sulfided $CoO–MoO_3/Al_2O_3$ catalysts with Co/Mo molar ratios of 0.23 and 0.47, respectively. In both cases, the catalyst precursors were calcined after impregnation with Mo and Co salts; this is different from the current study in which the $Co–MoO_3/Al_2O_3$ catalysts were calcined only after impregnation with $(NH_4)_6Mo_7O_{24}{\cdot}4H_2O$ in order to be consistent with the preparation of $Co–Mo_2C/Al_2O_3$ catalysts. Consistent with these authors, the ν_{CO} absorbance at 2105 cm^{-1} is assigned to CO adsorbed to Mo sites while the ν_{CO} absorbance at 2062 cm^{-1} is assigned to Co–Mo sites of the “Co–Mo–S” phase. Based on their

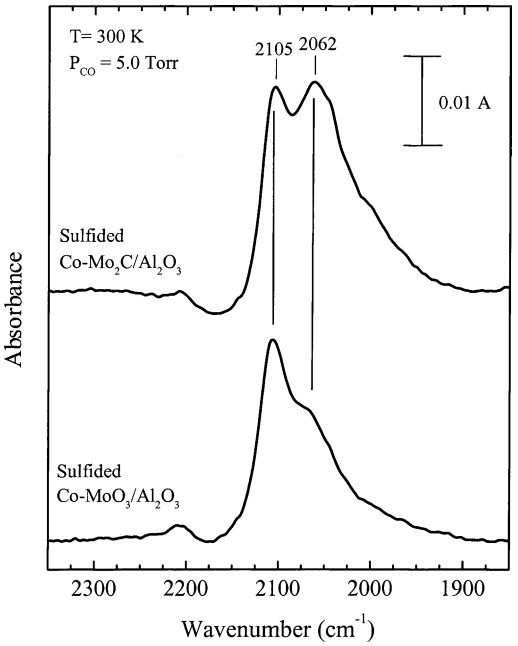

Fig. 11. IR spectra of adsorbed CO on Co-promoted Mo_2C/Al_2O_3 and MoO_3/Al_2O_3 catalysts with a Co/Mo ratio = 0.15. The catalysts were sulfided, then reduced prior to CO exposure at 295 K.

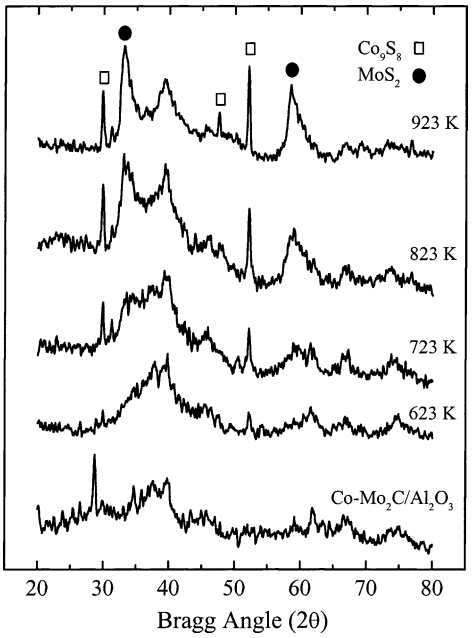

Fig. 12. XRD patterns for Co–Mo_2C/Al_2O_3 catalysts (8 wt.% Co, 48 wt.% Mo_2C, Co/Mo = 0.28) subjected to sulfidation pretreatments at the listed temperatures.

IR studies, Maugé and Lavalley [61] concluded that only 10% of the cobalt added to the catalyst formed promoted Co–Mo sites, with the remaining Co either associated with the alumina support or as sulfided Co species. Bachelier et al. [60] and Maugé and Lavalley [61] assigned a ν_{CO} absorbance at 2051 cm^{-1} to CO adsorbed to sites on a sulfided Co phase. Inspection of the IR spectrum of the sulfided Co–MoO_3/Al_2O_3 catalyst in Fig. 11 reveals a shoulder at ~2050 cm^{-1} that we assign to CO adsorbed to sulfided Co species.

Focusing now on the IR spectrum of adsorbed CO on the sulfided Co–Mo_2C/Al_2O_3 catalyst (Co/Mo = 0.15) (see Fig. 11), the same ν_{CO} absorbances as those observed on the sulfided Co–MoO_3/Al_2O_3 catalyst are apparent. As observed for unpromoted Mo_2C/Al_2O_3 catalysts, the IR spectrum indicates that the surface of Co–Mo_2C/Al_2O_3 catalysts is susceptible to sulfidation and the adsorption sites on these catalysts are indistinguishable by IR spectroscopy from those on conventional sulfide catalysts. However, comparison of the IR spectra of adsorbed CO on the Co–Mo_2C/Al_2O_3 and Co–MoO_3/Al_2O_3 catalysts reveals differences in spectral intensity. Relative to the ν_{CO} absorbance for unpromoted Mo sites, the ν_{CO} absorbance associated with promoted Co–Mo sites is larger on the sulfided Co–Mo_2C/Al_2O_3 catalyst than on the sulfided Co–MoO_3/Al_2O_3 catalyst. Taken together with the HDS activity data plotted in Fig. 10, these IR spectroscopic results suggest that Mo_2C/Al_2O_3 catalysts are more efficiently promoted by addition of $Co(NO_3)_2{\cdot}6H_2O$ than are MoO_3/Al_2O_3 catalysts. Thus, while the maximum in HDS activity is observed at a Co/Mo molar ratio of 0.50 for the Co–MoO_3/Al_2O_3 catalysts, less Co is needed for the Co–Mo_2C/Al_2O_3 catalysts which show a maximum in HDS activity at Co/Mo = 0.15.

For the Co–Mo_2C/Al_2O_3 and Co–MoO_3/Al_2O_3 catalysts, both similarities and differences are observed concerning the effects of a sulfidation pretreatment on the HDS catalytic properties of these materials relative to the unpromoted catalysts. Shown in Fig. 12 are the XRD patterns for a freshly prepared, high loading Co–Mo_2C/Al_2O_3 (8 wt.% Co, 48 wt.% Mo_2C, Co/Mo = 0.28), as well as samples of the catalyst sulfided at the indicated temperatures. The freshly prepared catalyst shows XRD peaks

associated with γ-Al_2O_3 and β-Mo_2C (see Fig. 7), as well as a strong peak at 28.7° which we tentatively assign to α-$CoMoO_4$ (card no. 25-1434 [59]). The assignment of this peak to α-$CoMoO_4$ is made with hesitation, but the oxide is apparently formed during the passivation of the catalyst following impregnation with cobalt nitrate and vacuum drying. If the Co–Mo_2C/Al_2O_3 catalysts were not passivated following the drying step, rapid, deep oxidation of the promoted carbide particles occurred. While the XRD pattern of the freshly prepared catalyst shows the presence of β-Mo_2C on the support, some of the Mo in the passivation layer is apparently present in the form of α-$CoMoO_4$. Upon sulfidation of the Co–Mo_2C/Al_2O_3 catalyst at 623 K and higher, the peak at 28.7° disappears and new peaks assigned to Co_9S_8 (card no. 19-0364 [59]) and MoS_2 (card no. 17-044 [59]) appear at 623 and 723 K, respectively. As determined by XRD, the formation of MoS_2 begins at a lower temperature and takes place to a greater extent for the Co–Mo_2C/Al_2O_3 catalyst (see Fig. 12) than was observed for the Mo_2C/Al_2O_3 catalyst (see Fig. 7). It is important to note, however, that in the temperature range typical of HDS processing (623–723 K), peaks assigned to β-Mo_2C remain in the XRD patterns.

Given the somewhat different sulfidation behavior of Co–Mo_2C/Al_2O_3 catalysts relative to unpromoted Mo_2C/Al_2O_3 catalysts, it is of interest to investigate the effect of the sulfidation temperature on the HDS activity of the promoted carbide catalysts. Despite the more pronounced formation of crystalline sulfides on the Co–Mo_2C/Al_2O_3 catalysts, the HDS activity data plotted in Fig. 13 show Co–Mo_2C/Al_2O_3 catalysts (Co/Mo = 0.31) to be significantly more active than Co–MoO_3/Al_2O_3 catalysts (Co/Mo = 0.31) for sulfidation temperatures in the range of 400–850 K. For a typical sulfidation temperature of 650 K, the Co–Mo_2C/Al_2O_3 catalyst is 21% more active than the Co–MoO_3/Al_2O_3 catalyst. These HDS activity results closely parallel those described earlier for the unpromoted Mo_2C/Al_2O_3 and MoO_3/Al_2O_3 catalysts.

Understanding the higher thiophene HDS activities of Co–Mo_2C/Al_2O_3 catalysts relative to their Co–MoO_3/Al_2O_3 counterparts is more difficult than for the unpromoted catalysts for which the higher HDS activity of the Mo_2C/Al_2O_3 catalysts was traced to a higher site density than for the MoO_3/Al_2O_3 catalysts as discussed above. For the promoted

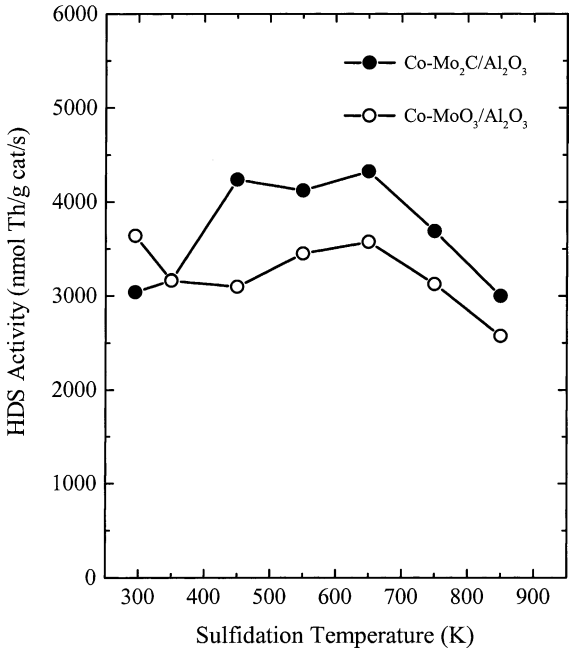

Fig. 13. Thiophene HDS activities for Co-promoted Mo_2C/Al_2O_3 and MoO_3/Al_2O_3 catalysts (Co/Mo = 0.31) as a function of the sulfidation pretreatment temperature.

catalysts, a similar conclusion cannot be drawn as the Co–Mo_2C/Al_2O_3 catalysts do not have consistently higher CO chemisorption capacities than do the Co–MoO_3/Al_2O_3 catalysts, but this result is not necessarily surprising. In contrast to sulfided Mo_2C/Al_2O_3 and MoO_3/Al_2O_3 catalysts, which expose one kind of adsorption site at their surfaces (see Fig. 5), the IR spectra of adsorbed CO on sulfided Co–Mo_2C/Al_2O_3 and Co–MoO_3/Al_2O_3 catalysts (see Fig. 11) reveal that at least three kinds of adsorption sites exist on their surfaces, complicating attempts to correlate HDS activities with chemisorption capacities for the promoted catalysts. Based upon the results presented in Figs. 10, 11 and 13, it appears that the Co–Mo_2C/Al_2O_3 catalysts more efficiently use the Co promoter, as the optimal Co/Mo ratio is lower than for the conventional Co–MoO_3/Al_2O_3 catalysts. Chianelli and Berhault [62] have recently implicated carbon as playing an important role in conventional sulfided Co–Mo catalysts in which a Co–Mo–C phase forms that is supported on Co and Mo sulfide phases. Based upon studies in which sulfide catalysts were prepared from carbon containing precursors, these

authors propose that a surface carbide phase is present under HDS conditions which is supported by the sulfide particles, essentially the reverse of the model proposed in our work (see Fig. 6). In the case of conventional sulfided Co–Mo catalysts, Chianelli and Berhault [62] suggest that significant amounts of carbon are incorporated into the surface region of the catalyst during sulfidation with sulfiding agents such as dimethyl disulfide, or by replacement of labile sulfur with carbon from the reactor feed [62,63]. While it is unclear how such a phase can be identified at present, it is possible that the substantial carbon content of the Co–Mo_2C/Al_2O_3 catalysts studied in our research facilitates formation of a high HDS activity Co–Mo–C surface phase under reaction conditions, but which is indistinguishable from the "Co–Mo–S" phase by IR spectroscopy of adsorbed CO. The presence of such a phase at the surface of the sulfided Co–Mo_2C/Al_2O_3 catalysts may explain their higher HDS activities relative to the sulfided Co–MoO_3/Al_2O_3 catalysts.

Based upon the high HDS activities measured for Co-promoted Mo_2C/Al_2O_3 and Mo_2N/Al_2O_3 catalysts, we investigated alternative methods of cobalt (and nickel) addition to Mo carbide and nitride catalysts by preparing alumina-supported bimetallic carbide and nitride materials. A preliminary report on this research described the synthesis of a Co_3Mo_3N/Al_2O_3 catalyst containing a significant Co metal or Co–N impurity phase [24]; this bimetallic nitride catalyst, when subjected to a sulfidation pretreatment, was observed to have a thiophene HDS activity nearly three times higher than that of a Mo_2N/Al_2O_3 catalyst having a similar Mo loading. In the current study, we describe HDS activity results for phase pure, alumina-supported Ni_2Mo_3N, Co_3Mo_3N and Co_3Mo_3C catalysts. The catalytic studies were initiated by investigating the effect of He degas only, reduction and sulfidation pretreatments on the thiophene HDS activity of a 20 wt.% Ni_2Mo_3N/Al_2O_3 catalyst. As shown in Fig. 14, the pretreatment utilized strongly affects the HDS activity of the 20 wt.% Ni_2Mo_3N/Al_2O_3 catalyst with the sulfided catalyst 1.3 and 3.6 times more active than the catalysts subjected to He degas only and reduction pretreatments, respectively. These observations are consistent with those we reported earlier for an impure Co_3Mo_3N/Al_2O_3 catalyst as well as the results of Ihm et al. [64] for unsupported Co_3Mo_3N; both studies found a sulfidation pretreatment to increase the HDS activity of the bimetallic nitride. The higher HDS activities realized for bimetallic nitride catalysts subjected to a sulfidation pretreatment (instead of a reduction pretreatment) may be due to the fact that sulfidation more effectively removes the thin oxide layer formed on the catalyst following synthesis than does reduction.

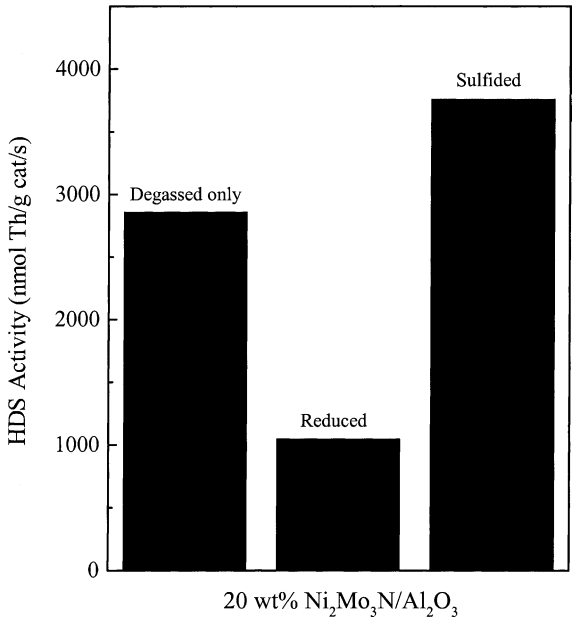

Fig. 14. A comparison of thiophene HDS activities for 20 wt.% Ni_2Mo_3N/Al_2O_3 catalysts subjected to degas only, reduction, and sulfidation pretreatments.

Shown in Fig. 15 are the XRD patterns for a freshly prepared 30 wt.% Ni_2Mo_3N/Al_2O_3 catalyst and samples of this same catalyst and of a $Ni_2Mo_3O_x/Al_2O_3$ catalyst each sulfided at 650 K. Peaks associated with Ni_2Mo_3N remain in the XRD pattern of the sulfided Ni_2Mo_3N/Al_2O_3 catalyst, but at reduced intensity. New peaks associated with the formation of MoS_2 crystallites on the catalyst surface are apparent; these same peaks are found in the XRD pattern of the sulfided $Ni_2Mo_3O_x/Al_2O_3$ catalyst. The XRD peaks due to MoS_2 are noticeably stronger for the Ni_2Mo_3N/Al_2O_3 catalyst sulfided at 650 K than for the Co–Mo_2C/Al_2O_3 catalyst sulfided at the higher temperature of 723 K. This may be due to the relatively low nitrogen content of Ni_2Mo_3N (17 at.% N vs. 33 at.% C in β-Mo_2C), as a higher content of the

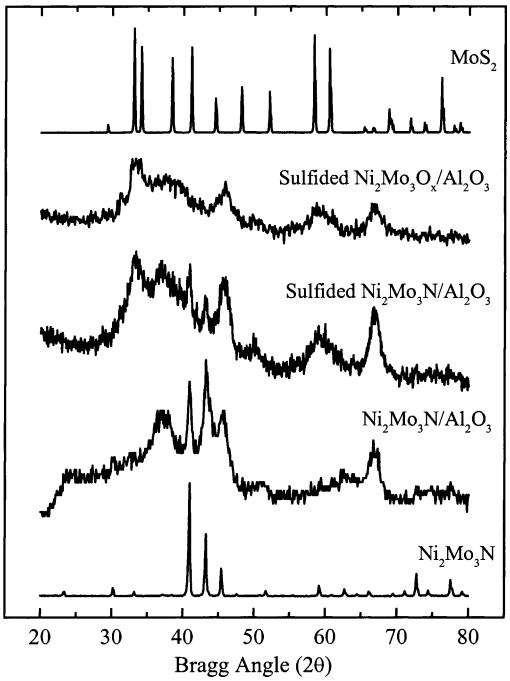

Fig. 15. XRD patterns for a passivated 30 wt.% Ni_2Mo_3N/Al_2O_3 catalyst, and for Ni_2Mo_3N/Al_2O_3 and $Ni_2Mo_3O_x/Al_2O_3$ catalysts sulfided at 650 K.

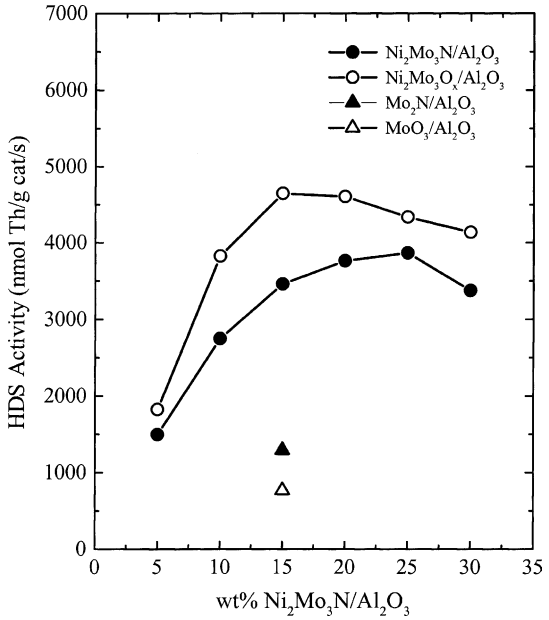

Fig. 16. Thiophene HDS activities for sulfided Ni_2Mo_3N/Al_2O_3 (5–30 wt.% Ni_2Mo_3N) and $Ni_2Mo_3O_x/Al_2O_3$ catalysts. The HDS activities for Mo_2N/Al_2O_3 and MoO_3/Al_2O_3 catalysts (21 wt.% MoO_3), sulfided under identical conditions, are also shown.

main group element could increase the resistance of the material to sulfidation. In any case, it is clear that formation of a sulfided Ni–Mo phase at the surface of the supported Ni_2Mo_3N particles has a beneficial effect on the HDS activity of Ni_2Mo_3N/Al_2O_3 catalysts.

The thiophene HDS activities of sulfided Ni_2Mo_3N/Al_2O_3 catalysts with a wide range of loadings are plotted as a function of the Ni_2Mo_3N loading in Fig. 16. The catalysts exhibit a trend of smoothly increasing HDS activity with a maximum reached for a loading of 25 wt.% Ni_2Mo_3N. Also plotted in Fig. 16 are the HDS activities of sulfided Mo_2N/Al_2O_3 and MoO_3/Al_2O_3 catalysts having similar Mo loadings (16 wt.% Mo_2N and 21 wt.% MoO_3, respectively), and of sulfided $Ni_2Mo_3O_x/Al_2O_3$ catalysts having the same metal loadings as the Ni_2Mo_3N/Al_2O_3 catalysts. The loadings of the Mo_2N/Al_2O_3 and MoO_3/Al_2O_3 catalysts are close to the optimal loadings determined in an earlier thiophene HDS study [7]. The sulfided 25 wt.% Ni_2Mo_3N/Al_2O_3 catalyst is 2.7 times more active than the sulfided 16 wt.% Mo_2N/Al_2O_3 catalyst, clearly indicating that incorporation of Ni into Mo nitride in the form of alumina-supported Ni_2Mo_3N catalysts results in a substantial increase in HDS activity. However, the Ni_2Mo_3N/Al_2O_3 catalysts are uniformly less active than the sulfided $Ni_2Mo_3O_x/Al_2O_3$ catalysts prepared from the oxidic precursors of the bimetallic nitride catalysts. Park et al. [23] reported a nitrided Ni–Mo/Al_2O_3 catalyst (Ni/Mo = 0.48) subjected to a reduction pretreatment (H_2, 673 K, 2 h) to be approximately 10% less active than a nitrided Mo/Al_2O_3 catalyst pretreated similarly. This apparent discrepancy with our results can be traced to the fact that Park et al. [23] used a reduction pretreatment that we have shown leads to a lower activity for Ni_2Mo_3N/Al_2O_3 catalysts (see Fig. 14), and possibly to the fact the Ni/Mo molar ratio these researchers used would not yield phase pure Ni_2Mo_3N on the alumina support. No XRD peaks other than those of the alumina support were observed for the nitrided Ni–Mo/Al_2O_3 catalyst.

Thiophene HDS activity measurements were also carried out for 20 wt.% Co_3Mo_3N/Al_2O_3 and Co_3Mo_3C/Al_2O_3 catalysts. As described above, we

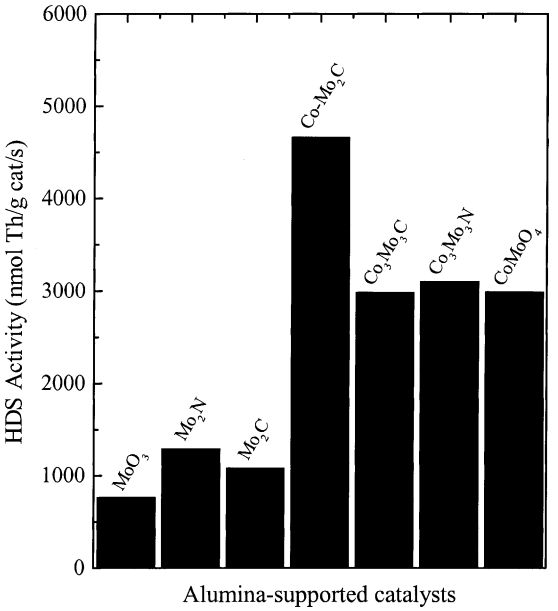

Fig. 17. A comparison of thiophene HDS activities for sulfided 20 wt.% Co_3Mo_3N/Al_2O_3, 20 wt.% Co_3Mo_3C/Al_2O_3 and $CoMoO_4/Al_2O_3$ (25.4 wt.% $CoMoO_4$) catalysts. For comparison purposes, also shown are the HDS activities for MoO_3/Al_2O_3, Mo_2N/Al_2O_3, Mo_2C/Al_2O_3, and Co–Mo_2C/Al_2O_3 catalysts, all subjected to a sulfidation pretreatment at 650 K.

previously observed an impure Co_3Mo_3N/Al_2O_3 catalyst subjected to a sulfidation pretreatment to have an HDS activity nearly three times higher than that of a Mo_2N/Al_2O_3 catalyst subjected to a reduction pretreatment [24]. The HDS activities of phase pure 20 wt.% Co_3Mo_3N/Al_2O_3 and Co_3Mo_3C/Al_2O_3 catalysts are shown in Fig. 17 along with the activities of a number of other catalysts for comparison purposes; all the catalysts were subjected to a sulfidation pretreatment at 650 K. The 20 wt.% Co_3Mo_3N/Al_2O_3 and Co_3Mo_3C/Al_2O_3 catalysts were found to be 2.4 and 2.7 times more active than 16 wt.% Mo_2N/Al_2O_3 and Mo_2C/Al_2O_3 catalysts, respectively, showing that incorporation of Co into bimetallic nitride and carbide phases with Mo results in substantially higher HDS activities for the catalysts. The extent of the HDS activity increase for the 20 wt.% Co_3Mo_3N/Al_2O_3 and Co_3Mo_3C/Al_2O_3 catalysts is similar to that observed for a 25 wt.% Ni_2Mo_3N/Al_2O_3 catalyst, but substantially less than that realized for the optimally promoted Mo carbide catalyst, Co–Mo_2C/Al_2O_3 (Co/Mo = 0.15), for which a 4.5-fold increase in HDS activity was measured.

There are a number of possible explanations for the lower HDS activity of the bimetallic carbide and nitride catalysts relative to the promoted Mo carbide catalysts. One is the fact that the Co/Mo molar ratio is fixed by stoichiometry to 1.0 for Co_3Mo_3N/Al_2O_3 and Co_3Mo_3C/Al_2O_3 catalysts and at Ni/Mo = 0.67 for the Ni_2Mo_3N/Al_2O_3 catalysts, while the optimal Co/Mo ratio for the Co–Mo_2C/Al_2O_3 catalysts was found to be 0.15. For the Co–Mo_2C/Al_2O_3 catalyst with Co/Mo = 1.0, the HDS activity is 20% lower than for the optimally promoted catalyst. Other possible explanations for the low HDS activity enhancement associated with the incorporation of Co or Ni in bimetallic nitride and carbide phases are the low N (or C) content of these catalysts relative to the monometallic carbide and nitride catalysts as discussed above for Ni_2Mo_3N/Al_2O_3 catalysts, and the method of Co and Ni incorporation. Focusing on this latter possibility, the effect of Co incorporation into bimetallic phases can be examined by comparing not only Co–Mo_2C/Al_2O_3 (Co/Mo = 1.0) and Co_3Mo_3C/Al_2O_3 catalysts but also Co–MoO_3/Al_2O_3 (Co/Mo = 1.0) and $CoMoO_4/Al_2O_3$ catalysts. In both cases the formation of bimetallic phases is unfavorable with respect to HDS activity. For catalysts sulfided under identical conditions, the Co–Mo_2C/Al_2O_3 catalyst (Co/Mo = 1.0) is 26% more active than the Co_3Mo_3C/Al_2O_3 catalyst, and the Co–MoO_3/Al_2O_3 catalyst (Co/Mo = 1.0) is 22% more active than the $CoMoO_4/Al_2O_3$ catalyst. These results clearly show that Co promotion is the preferred method of incorporating the second metal into both the conventional sulfide catalysts and the carbide catalysts. The results for the conventional catalysts are consistent with the research of others [65].

4. Conclusions

Alumina-supported monometallic, bimetallic and promoted carbide and nitride catalysts have been prepared and their HDS catalytic properties have been investigated. Alumina-supported β-Mo_2C and γ-Mo_2N catalysts have been observed to be significantly more active than sulfided MoO_3/Al_2O_3 catalysts, and XRD and chemisorption studies of

the Mo_2C/Al_2O_3 catalysts indicate that they exhibit strong resistance to deep sulfidation. Cobalt promoted catalysts, $Co–Mo_2C/Al_2O_3$, have been observed to be substantially more active than conventional sulfided $Co–MoO_3/Al_2O_3$ catalysts while requiring less Co to achieve optimal HDS activity. Alumina-supported bimetallic nitride and carbide catalysts (Ni_2Mo_3N/Al_2O_3, Co_3Mo_3N/Al_2O_3, Co_3Mo_3C/Al_2O_3), while significantly more active for thiophene HDS than unpromoted Mo nitride and carbide catalysts, are less active than conventional sulfided Ni–Mo and Co–Mo catalysts prepared from the same oxidic precursors.

Acknowledgements

This research was supported by the National Science Foundation under grant number CHE-9610438. Acknowledgment is also made to the Henry Dreyfus Teacher-Scholar Awards Program of the Camille and Henry Dreyfus Foundation for partial support of this research.

References

[1] H. Topsøe, B. Clausen, F.E. Massoth, in: J.R. Anderson, M. Boudart (Eds.), Catalysis: Science and Technology, vol. 11, Springer, Berlin, 1996, p. 1.
[2] T. Kabe, A. Ishihara, W. Qian, Hydrodesulfurization and Hydrodenitrogenation: Chemistry and Engineering, Wiley, Weinheim, 1999.
[3] J.S. Lee, M. Boudart, Appl. Catal. 19 (1985) 207.
[4] S. Ramanathan, S.T. Oyama, J. Phys. Chem. 99 (1995) 16365.
[5] P.A. Aegerter, W.W.C. Quigley, G.J. Simpson, D.D. Ziegler, J.W. Logan, K.R. McCrea, S. Glazier, M.E. Bussell, J. Catal. 164 (1996) 109.
[6] D.J. Sajkowski, S.T. Oyama, Appl. Catal. A 134 (1996) 339.
[7] K.R. McCrea, J.W. Logan, T.L. Tarbuck, J.L. Heiser, M.E. Bussell, J. Catal. 171 (1997) 255.
[8] G.M. Dolce, P.E. Savage, L.T. Thompson, Energy Fuels 11 (1997) 668.
[9] B. Dhandapani, T.S. Clair, S.T. Oyama, Appl. Catal. A 168 (1998) 219.
[10] M. Nagai, T. Miyao, T. Tuboi, Catal. Lett. 18 (1993) 9.
[11] M. Nagai, O. Uchino, T. Kusgaya, S. Omi, in: G. Froment, B. Delmon, P. Grange (Eds.), Hydrotreatment and Hydrocracking of Oil Fractions, Elsevier, New York, 1997, p. 541.
[12] M. Nagai, M. Kiyoshi, H. Tominaga, S. Omi, Chem. Lett. (2000) 702.
[13] R.L. Levy, M. Boudart, Science 181 (1973) 547.
[14] M. Boudart, A.W. Aldag, L.D. Ptak, J.E. Benson, J. Catal. 11 (1968) 35.
[15] S.T. Oyama (Ed.), The Chemistry of Transition Metal Carbide and Nitrides, Blackie, New York, 1996, p. 1.
[16] M.E. Eberhart, J.M. MacLaren, in: S.T. Oyama (Ed.), The Chemistry of Transition Metal Carbide and Nitrides, Blackie, New York, 1996, p. 106.
[17] S.T. Oyama, Catal. Today 15 (1992) 172.
[18] S.T. Oyama, G.L. Haller, in: G.C. Bond, G. Webb (Eds.), Catalysis, vol. 5, The Royal Society of Chemistry, London, 1982, p. 333.
[19] S.T. Oyama (Ed.), The Chemistry of Transition Metal Carbides and Nitrides, Blackie, New York, 1996.
[20] T.A. Pecoraro, R.R. Chianelli, J. Catal. 67 (1981) 430.
[21] J.P.R. Vissers, C.K. Groot, E.M. van Oers, V.H.J. de Beer, R. Prins, Bull. Soc. Chim. Belg. 93 (1984) 813.
[22] M.J. Ledoux, O. Michaux, G. Agostini, J. Catal. 102 (1986) 275.
[23] H.K. Park, J.K. Lee, J.K. Yoo, E.S. Ko, D.S. Kim, K.L. Kim, Appl. Catal. A 150 (1997) 21.
[24] J.W. Logan, J.L. Heiser, K.R. McCrea, B.D. Gates, M.E. Bussell, Catal. Lett. 56 (1998) 165.
[25] J. Trawczynski, Appl. Catal. A 197 (2000) 289.
[26] S. Korlann, B. Diaz, M.E. Bussell, Chem. Mater. 14 (2002) 4049.
[27] A.L. Diaz, M.E. Bussell, J. Phys. Chem. 97 (1993) 470.
[28] N. Arul Dhas, A. Gedanken, Chem. Mater. 9 (1997) 3144.
[29] F. Solymosi, R. Nemeth, L. Ovari, L. Egri, J. Catal. 195 (2000) 316.
[30] S. Naito, M. Tsuji, T. Miyao, Catal. Today 77 (2002) 161.
[31] F. Solymosi, A. Erdohelyi, A. Szoke, Catal. Lett. 32 (1995) 43.
[32] S. Yuan, S. Bee Derouane-Abd Hamid, Y. Li, P. Ying, Q. Xin, E. Derouane, C. Li, J. Mol. Catal. A 184 (2002) 257.
[33] D. Mordenti, D. Brodzki, G. Djega-Mariadassou, J. Solid State Chem. 141 (1998) 114.
[34] C. Sayag, S.S.J. Trawczynski, G. Djega-Mariadassou, Fuel Process. Technol. 77–78 (2002) 261.
[35] M. Nagai, J. Takada, S. Omi, J. Phys. Chem. B 103 (1999) 10180.
[36] A. Guerrero-Ruiz, M. Zhang, B. Bachiller-Baeza, I. Rodriguez-Ramos, Catal. Lett. 55 (1998) 165.
[37] C. Suryanarayana, M.G. Norton, X-ray Diffraction: A Practical Approach, Plenum Press, New York, 1998.
[38] J.S. Lee, K.H. Lee, J.Y. Lee, J. Phys. Chem. 96 (1992) 362.
[39] T. Miyao, I. Shishikura, M. Matsuoka, M. Nagai, S.T. Oyama, Appl. Catal. A 165 (1997) 419.
[40] M. Nagai, K. Oshikawa, T. Kurakami, T. Miyao, S. Omi, J. Catal. 180 (1998) 14.
[41] S. Yang, C. Li, Q. Xin, Chem. Commun. (1997) 13.
[42] S. Yang, C. Li, J. Xu, Q. Xin, J. Phys. Chem. B 102 (1998) 6986.
[43] Z. Wu, Y. Chu, S. Yang, Z. Wei, C. Li, Q. Xin, J. Catal. 194 (2000) 23.
[44] M. Nagai, A. Irisawa, S. Omi, J. Phys. Chem. B 102 (1998) 7619.
[45] K. Hada, M. Nagai, S. Omi, J. Phys. Chem. B 104 (2000) 2090.

[46] M.E. Bussell, P. Mills, B.P. Woodruff, R. Main, D.C. Phillips, Prepr. Pap. Am. Chem. Soc. Div. Pet. Chem. 44 (1999) 206.
[47] S. Yang, X. Jiang, W. Yan, P. Ying, Q. Xin, Chin. J. Catal. 18 (1997) 179.
[48] Y. Chu, Z. Wei, S. Yang, C. Li, Q. Xin, E. Min, Appl. Catal. A 176 (1999) 17.
[49] K. Miga, K. Stanczyk, C. Sayag, D. Brodzki, G. Djega-Mariadassou, J. Catal. 193 (1999) 63.
[50] W. Yuhong, L. Wei, Z. Minghui, G. Naijia, T. Keyi, Appl. Catal. A 215 (2001) 39.
[51] D.S. Bem, C.P. Gibson, H.-C. zur Loye, Chem. Mater. 5 (1993) 397.
[52] K.S. Weil, P.N. Kumta, Mater. Sci. Eng. B 38 (1996) 109.
[53] S. Alconchel, F. Sapiña, D. Beltrán, A. Beltrán, J. Mater. Chem. 8 (1998) 1901.
[54] P.S. Herle, M.S. Hegde, K. Sooryanarayana, T.N.G. Row, G.N. Subbanna, Inorg. Chem. 37 (1998) 4128.
[55] S. Alconchel, F. Sapiña, D. Beltrán, A. Beltrán, J. Mater. Chem. 9 (1999) 749.
[56] C.J.H. Jacobsen, Chem. Commun. (2000) 1057.
[57] S. Yang, Y. Li, J. Xu, C. Li, Q. Xin, I. Rodriguez-Ramos, A. Guerrero-Ruiz, Phys. Chem. Chem. Phys. 2 (2000) 3313.
[58] P. Mills, D.C. Phillips, B.P. Woodruff, R. Main, M.E. Bussell, J. Phys. Chem. B 104 (2000) 3237.
[59] JCPDS Powder Diffraction File, International Centre for Diffraction Data, Swarthmore, PA, 2000.
[60] J. Bachelier, M.J. Tilliette, M. Cornac, J.C. Duchet, J.C. Lavalley, D. Cornet, Bull. Soc. Chim. Belg. 93 (1984) 743.
[61] F. Maugé, J.C. Lavalley, J. Catal. 137 (1992) 69.
[62] R.R. Chianelli, G. Berhault, Catal. Today 53 (1999) 357.
[63] G. Berhault, A. Mehta, A.C. Pavel, J. Yang, L. Rendon, M.J. Yacaman, L. Cota Araiza, A. Duarte Moller, R.R. Chianelli, J. Catal. 198 (2001) 9.
[64] S.-K. Ihm, D.-W. Kim, D.-K. Lee, in: C.H. Bartholomew, G.A. Fuentes (Eds.), Studies in Surface Science and Catalysis, vol. 111, Elsevier, New York, 1997, p. 343.
[65] J.A.R. van Veen, E. Gerkema, A.M. van der Kraan, P.A.J.M. Hendriks, H. Beens, J. Catal. 133 (1992) 112.